Reaction rate kernel for dichotomous noise-induced transitions in bistable systems

Ivan L'Heureux

Ottawa-Carleton Institute for Physics, University of Ottawa, Ottawa, Ontario, Canada K1N 6N5

We present a study of the kinetics of transitions between two stochastic states induced by external dichotomous noise in deterministic bistable one-variable systems. The time dependence of the rate kernel describing the transition is studied by relating the kernel to the spectrum of the stochastic dynamical operator projected onto fast time scales. The formalism is applied to an exactly solvable case (the piecewise quadratic potential) and numerically to a quartic potential. This analysis is useful for the study of memory effects in fast reaction rate processes.

I. INTRODUCTION

Bistable dissipative systems abound in nature [1–3]. These are characterized by the coexistence of two attractors for a given set of control parameter values. When nonlinear systems are subjected to external noise, interesting dynamical behavior may arise. Under stochastic dynamics, new states may be created which have no deterministic counterpart [4,5]. Moreover, if many states coexist, transitions from one state to another may be induced as the phase point wanders randomly from one basin of attraction to another [6]. It is of interest to investigate the kinetics of such noise-induced transitions.

In this paper, we consider simple one-variable dissipative systems which can be described in terms of a deterministic bistable potential. The systems are driven by additive dichotomous noise, which is characterized by an amplitude Δ and a noise correlation time γ^{-1}. This description may be used to model far-from-equilibrium noise-induced transitions in chemical systems, lasers, or nonlinear optical devices [4,6–8].

For a wide range of the noise parameter values, it is known [6] that the kinetics of such noise-induced transitions is analogous to the kinetics of isomerization reactions between two chemical species. In the noise-induced rate process, the deterministic basins of attraction may be identified as distinct "chemical species" that "react" under the effect of the random fluctuations driving the system. If the relaxation time of the species population numbers is much larger than all other time scales in the model, then the dynamics of the population numbers obeys a simple phenomenological law characterized by a first-order rate coefficient. Direct simulations techniques have been used [9] to compute explicitly the rate coefficient. The results are consistent with those obtained from a first passage time formulation [10–13].

In general, however, such a clear separation of time scales is not valid. This is typically the case when the ratio of the potential barrier height with the noise strength (defined as Δ^2/γ) is small. In this case, the decay of the population numbers follows a generalized rate law which is nonlocal in time ("memory effects").

It has been previously shown [14] that these effects may in principle be investigated by determining the eigenvalues and eigenfunctions of the stochastic dynamical operator. However, such an approach may have a limited use since a large number of spectral components must be determined in order to obtain convergent results, even at relatively large times. In order to circumvent these difficulties, a different spectral method may be developed to investigate the memory effects. This method relies on the spectrum of the stochastic dynamical operator *projected* onto the small time scales and was first applied to the cases where a bistable system is subjected to white Gaussian noise [15] or Bhatnagar-Gross-Krook kinetics [16,17]. In this paper, we apply such an approach to dichotomous noise.

The paper is divided as follows. In Sec. II we present the basic formalism. The derivation of the generalized rate law is reviewed. It is seen that the memory effects may be described in terms of an integrated rate kernel $K(t)$. We discuss the spectral properties of the projected stochastic operator and show explicitly that $-\gamma$ is an eigenvalue and that 0 is a doubly degenerate eigenvalue. We also relate the rate kernel to this spectrum. In Sec. III we consider an exactly solvable case: the piecewise quadratic potential. The model is presented and an outline of the solution to the eigenvalue problem is given. Two different situations are discussed: a high barrier and a low barrier case. In Sec. IV we present a numerical approach to solve the eigenvalue problem for the quartic potential. Two similar cases are again discussed. Finally, concluding remarks are given in Sec. V. Two appendixes complete the analysis.

II. BASIC FORMALISM

A. Integrated rate kernel

We consider a single dynamical variable $x(t)$ obeying the overdamped dynamics:

$$\dot{x} = f(x) + I(t) . \tag{2.1}$$

The deterministic part of the evolution derives from a potential exhibiting bistability $f(x) \equiv -dV/dx$. Two stable fixed point x_A, x_B coexist separated by an unstable one at

x_0. In Eq. (2.1), $I(t)$ is an external Poisson dichotomous noise process: it takes one of two discrete values $\pm\Delta$ with a Poisson distributed transition time [4,18–20]. The statistical properties of this stochastic forcing are described by

$$\langle I(t)\rangle=0, \quad \langle I(t)I(t+\tau)\rangle=\Delta^2\exp(-\gamma|\tau|) , \qquad (2.2)$$

where Δ is the amplitude of the noise and γ is twice the mean frequency of transition $\pm\Delta\to\mp\Delta$. The evolution equation for the probability density $p(x,\pm\Delta,t)\equiv p_\pm(x,t)$ in the extended phase space $\{x,I\}$ may be written as

$$\dot{\mathbf{p}}(x,t)=\mathbf{D}\cdot\mathbf{p}(x,t) , \qquad (2.3)$$

where the vector $\mathbf{p}(x,t)=(p_+(x,t),p_-(x,t))^T$ and the stochastic evolution operator is

$$\mathbf{D}=\begin{bmatrix} -\dfrac{\partial}{\partial x}[f(x)+\Delta]-\gamma/2 & \gamma/2 \\[3mm] \gamma/2 & -\dfrac{\partial}{\partial x}[f(x)-\Delta]-\gamma/2 \end{bmatrix} . \qquad (2.4)$$

The probability density contracted onto the dynamical variable x of interest is then

$$p(x,t)=p_+(x,t)+p_-(x,t) . \qquad (2.5)$$

The stationary probability density $p_s(x)=\lim_{t\to\infty}p(x,t)$ is easily found to be [4,18]

$$p_s(x)=\begin{cases} \dfrac{Z}{D_e(x)}\exp\displaystyle\int_{x_0}^x dx'f(x')/D_e(x'), & x\in\mathcal{M} \\[3mm] 0, & x\notin\mathcal{M} , \end{cases} \qquad (2.6)$$

where $D_e(x)=\Delta^2[1-f^2(x)/\Delta^2]/\gamma$ and Z is a constant. The implicit relations $f(M_{A,B})=\pm\Delta$ define the boundaries of the support $\mathcal{M}=[M_A,M_B]$. The stationary density is normalized in such a way that $\int_{M_A}^{M_B}dx\, p_s(x)=1$. The individual stationary densities $p_{s\pm}(x)$ are easily found by setting Eq. (2.3) equal to 0:

$$p_{s\pm}(x)=\tfrac{1}{2}p_s(x)[1\mp f(x)/\Delta] . \qquad (2.7)$$

If the noise amplitude and the noise frequency are sufficiently large, the stationary probability density vanishes at the support boundaries and is bimodal with a minimum at x_0 and maxima at the deterministic fixed points x_A,x_B [4,6]. It is this case that interests us here as we will use the formalism of reaction dynamics. An asymptotic analysis of the behavior of $p_s(x)$ near the boundaries of the support indicates that the stationary distribution is bimodal for

$$\gamma/2>\max(s_A,s_B) , \qquad (2.8)$$

where $s_A=-f'(M_A)>0$ and similarly for s_B.

We then define the instantaneous population number in the states A,B as

$$N_{A,B}(t)=\theta(\sigma_{A,B}(x_0-x(t))) , \qquad (2.9)$$

where $\theta(x)$ is the Heaviside step function and $\sigma_{A,B}=\pm 1$, respectively. This definition reflects the fact that whenever the dynamical variable is in the basin of attraction associated with one stable fixed point, it contributes to the corresponding population number. The nonequilibrium average population number is therefore

$$\overline{N}_{A,B}(t)=\int_{-\infty}^\infty p(x,t)\theta(\sigma_{A,B}(x_0-x(0)))dx . \qquad (2.10)$$

The overbar corresponds to a nonequilibrium average over the stochastic realizations. The stationary population numbers are

$$\eta_A=\int_{M_A}^{x_0}p_s(x)dx, \quad \eta_B=\int_{x_0}^{M_B}p_s(x)dx . \qquad (2.11)$$

We define the projector onto the population numbers [9] acting upon a function $g_i(x,t)$ (with $i=\pm$) as

$$\mathcal{P}g_i(x,t)=\left[\sum_j\int_{-\infty}^\infty dx\,\theta(x_0-x)g_j(x,t)\right]$$
$$\times\eta_A^{-1}\theta(x_0-x)p_{si}(x)$$
$$+\left[\sum_j\int_{-\infty}^\infty dx\,\theta(x-x_0)g_j(x,t)\right]$$
$$\times\eta_B^{-1}\theta(x-x_0)p_{si}(x) . \qquad (2.12)$$

We denote the complementary projector as $\mathcal{Q}\equiv 1-\mathcal{P}$. We assume that the initial distribution densities $p_i(x,0)$ are proportional to $p_{s,i}(x)$ in each region A or B so that $\mathcal{Q}p_i(x,0)=0$ [9]. Applying standard projection operator techniques on the stochastic evolution operator gives

$$\frac{\partial}{\partial t}\mathcal{P}\mathbf{p}(t)=\mathcal{P}\mathbf{D}\cdot\mathcal{P}\mathbf{p}(t)+\int_0^t d\tau\,\mathcal{P}\mathbf{D}\cdot e^{\mathcal{Q}D\tau}\cdot\mathcal{Q}\mathbf{D}\cdot\mathcal{P}\mathbf{p}(t-\tau) .$$

It is then easy to show [9] that the deviation of the population numbers from their equilibrium values

$$\delta\overline{N}_A(t)=\overline{N}_A(t)-\eta_A \qquad (2.13)$$

obeys a formally exact generalized rate law

$$\delta\dot{\overline{N}}_A(t)=-\int_0^t\Lambda(t-\tau)\delta\overline{N}_A(\tau)d\tau . \qquad (2.14)$$

A similar relation holds for $\overline{N}_B$. In Eq. (2.14), $\Lambda(t)$ denotes the rate kernel

$$\Lambda(t)=-\sum_{i,j,k,l}\int_{-\infty}^\infty dx\,\theta(x_0-x)$$
$$\times D_{ij}(e^{\mathcal{Q}Dt})_{jk}D_{kl}p_{sl}(x)u(x) , \qquad (2.15)$$

where

$$u(x)\equiv\theta(x_0-x)\eta_A^{-1}-\theta(x-x_0)\eta_B^{-1} . \qquad (2.16)$$

An equivalent formulation of the rate law can be obtained by integrating (2.14) with respect to time:

$$\delta\overline{N}_A(t)-\delta\overline{N}_A(0)=-\int_0^t K(\tau)\delta\overline{N}_A(t-\tau)d\tau , \qquad (2.17)$$

where the integrated rate kernel is

$$K(t)=\int_0^t\Lambda(t')dt' . \qquad (2.18)$$

When $\Lambda(t)$ has a short memory compared with the relaxation of the mean population number, the integrated rate kernel quickly reaches its asymptotic value $K(\infty)$. In this case, a simple phenomenological rate law $\delta \dot{\overline{N}}_A(t) \approx -k \delta \overline{N}_A(t)$ holds, with the rate coefficient $k = K(\infty) = \int_0^\infty \Lambda(\tau) d\tau$. In general however, this time-scale separation is not valid and a complete understanding of the population number dynamics requires the full knowledge of $K(t)$.

Finally, we express the integrated rate kernel in terms of projection operators. Using the facts that $\mathbf{D} \cdot \mathbf{p}_s = 0$, $d\theta(\pm(x_0 - x))/dx = \mp\delta(x - x_0)$, and x_0 is a deterministic fixed point $[f(x_0) = 0]$, it is easy to show that

$$\sum_{i,j} \int_{-\infty}^\infty dx \ \theta(x_0 - x) D_{ij} p_{sj}(x) u(x) = 0 . \tag{2.19}$$

Hence

$$\Lambda(t) = -\sum_{i,j,k,l} \int_{-\infty}^\infty dx \ \theta(x_0 - x) D_{ij} (e^{QDt})_{jk}$$
$$\times QD_{kl} p_{sl}(x) u(x) .$$

Therefore

$$K(t) = -\sum_{i,j,k} \int_{-\infty}^\infty dx \ \theta(x_0 - x) D_{ij} (e^{QDt})_{jk} p_{sk}(x) u(x) , \tag{2.20}$$

where we used the fact that $K(0) = 0$, as is seen from (2.19) or (2.18). Equation (2.20) can be written more compactly as

$$K(t) = -\sum_{i,j} \int_{-\infty}^\infty dx \ \theta(x_0 - x) D_{ij} \xi_j(x, t) , \tag{2.21}$$

where

$$\xi_j(x, t) = \sum_k (e^{QDt})_{jk} p_{sk}(x) u(x) . \tag{2.22}$$

The evolution of the integrated rate kernel can then be interpreted in terms of the dynamics of an auxiliary variable $\xi_i(x, t)$, which obeys the following *projected* dynamics:

$$\frac{\partial}{\partial t} \xi_i(x, t) = \sum_j QD_{ij} \xi_j(x, t) \tag{2.23}$$

with the initial condition

$$\xi_i(x, 0) = p_{si}(x) u(x) . \tag{2.24}$$

Note that $\xi_i(x, 0)$ is null for x outside the support $\mathcal{M}$.

B. Projected dynamics as an eigenvalue problem

In the preceding subsection, we saw that the dynamics of the integrated rate kernel is determined by the projected evolution operator QD [Eq. (2.23)]. In order to solve this problem, we consider the following eigenvalue problem. Let μ be the eigenvalue of the operator QD with right eigenvectors $\vec{\alpha} = (\alpha_+, \alpha_-)^T$:

$$QD \cdot \vec{\alpha}(x) = \mu \vec{\alpha}(x) . \tag{2.25}$$

Using $Q = 1 - \mathcal{P}$, the explicit form (2.12) of $\mathcal{P}$, and performing the integrals, the eigenvalue problem reduces to

$$(D_{++} - \mu)\alpha_+ + D_{+-}\alpha_- = -\Delta p_{s+}(x) Qu(x) ,$$
$$(D_{--} - \mu)\alpha_- + D_{-+}\alpha_+ = -\Delta p_{s-}(x) Qu(x) , \tag{2.26}$$

where

$$Q \equiv \alpha_+(x_0) - \alpha_-(x_0) . \tag{2.27}$$

$\alpha_\pm$ are both continuous at the unstable fixed point x_0.

It is necessary to introduce adjoint operators in order to obtain the left eigenvectors. An adjoint operator $\mathbf{A}^\dagger$ is defined on the support such that for two vectors $\mathbf{a}, \mathbf{b}$ we have

$$\langle \mathbf{b} | \mathbf{A} \cdot \mathbf{a} \rangle \equiv \sum_{i,j} \int_{M_A}^{M_B} dx \ b_i A_{ij} a_j = \sum_{i,j} \int_{M_A}^{M_B} dx \ (A_{ij}^\dagger b_j) a_i$$
$$= \langle \mathbf{A}^\dagger \cdot \mathbf{b} | \mathbf{a} \rangle .$$

The left eigenvectors $\vec{\beta} = (\beta_+, \beta_-)^T$ of QD are solved by the following eigenvalue problem:

$$(QD)^\dagger \cdot \vec{\beta}(x) = \mu \vec{\beta}(x) = \mathbf{D}^\dagger Q^\dagger \vec{\beta}(x) . \tag{2.28}$$

Here $\mathcal{D}^\dagger$ is the operator adjoint to $\mathbf{D}$,

$$\mathbf{D}^\dagger = \begin{bmatrix} (f+\Delta)\dfrac{\partial}{\partial x} - \gamma/2 & \gamma/2 \\[2mm] \gamma/2 & (f-\Delta)\dfrac{\partial}{\partial x} - \gamma/2 \end{bmatrix} , \tag{2.29}$$

and $Q^\dagger = 1 - \mathcal{P}^\dagger$, with

$$\mathcal{P}^\dagger(\cdots) = \theta(x_0 - x)\left[\sum_i \int_{M_A}^{M_B} dx \ \theta(x_0 - x) p_{si}(x)(\cdots)\eta_A^{-1}\right] + \theta(x - x_0)\left[\sum_i \int_{M_A}^{M_B} dx \ \theta(x - x_0) p_{si}(x)(\cdots)\eta_B^{-1}\right] . \tag{2.30}$$

In Eq. (2.30), it is understood that $M_A \leq x \leq M_B$.

Thus the left eigenvector problem takes the explicit form

$$(D_{++}^\dagger - \mu)\beta_+ + D_{+-}^\dagger \beta_- = -\Delta\delta(x - x_0)R ,$$
$$(D_{--}^\dagger - \mu)\beta_- + D_{-+}^\dagger \beta_+ = \Delta\delta(x - x_0)R , \tag{2.31}$$

where $R \equiv \int_{M_A}^{M_B} dx \ (\beta_+ p_{s+} + \beta_- p_{s-}) u(x)$. The left eigenvectors are thus determined by the *unprojected* adjoint evolution operator $\mathbf{D}^\dagger$ subjected to a discontinuity at the unstable fixed point

$$\beta_+(x_0^+) - \beta_+(x_0^-) = \beta_-(x_0^+) - \beta_-(x_0^-) = -R . \tag{2.32}$$

Here $x_0^{\pm} \equiv \lim_{\epsilon \to 0}(x_0 \pm \epsilon)$.

By transforming the quantity $\langle \vec{\beta} | Q\mathbf{D} \cdot \vec{\alpha} \rangle$, it is easy to see that $\{\vec{\alpha}, \vec{\beta}\}$ form a biorthogonal set of eigenfunctions. The normalization may be chosen so that

$$\langle \vec{\beta}^\mu | \vec{\alpha}^{\mu'} \rangle = \delta_{\mu, \mu'} \; . \tag{2.33}$$

Here the eigenvalue dependence has been explicitly written and the right-hand side is equal to one for $\mu = \mu'$ and zero otherwise. The orthogonalization condition is valid if the boundary terms resulting from the integration by parts in the transformation of $\langle \vec{\beta} | Q\mathbf{D} \cdot \vec{\alpha} \rangle$ vanish. Using the fact that $f(M_{A)} = \Delta$, this condition gives the following boundary conditions for the eigenfunctions:

$$\beta_+(M_A)\alpha_+(M_A) = \beta_-(M_B)\alpha_-(M_B) = 0 \; . \tag{2.34}$$

The behavior of the eigenfunctions near the boundaries of the support can easily be determined by an asymptotic analysis of the eigenvalue equations. We expand the deterministic force about $x = M_B$, say. We have to first order $f(x) = -\Delta + s_B \epsilon$, where $s_B \equiv -f'(M_B) > 0$ and $\epsilon \equiv M_B - x \ll 1$. We set the eigenfunctions proportional to $\epsilon^{y_\pm}$ near M_B, where $y_\pm$ are some numbers to be determined. We balance the terms with the smallest power of ϵ in the eigenvalue equations (2.26) and (2.31). We finally obtain the following behavior near M_B, consistent with the required boundary conditions (2.34) and the existence of a normalization (2.33): (i) for $\mathrm{Re}(\mu) > s_B - \gamma/2$,

$$\alpha_+ \sim \epsilon^{(\mu+\gamma/2)s_B^{-1}-1} \to 0 \; , \quad \alpha_- \sim \epsilon^{(\mu+\gamma/2)s_B^{-1}} \to 0 \; ,$$

$$\beta_+ \sim \mathrm{const} \; , \quad \beta_- \sim \mathrm{const} \; ;$$

(ii) for $-\gamma/2 < \mathrm{Re}(\mu) < s_B - \gamma/2$, two families of solutions exist,

$$\alpha_+ \sim \epsilon^{(\mu+\gamma/2)s_B^{-1}-1} \to \infty \; , \quad \alpha_- \sim \epsilon^{(\mu+\gamma/2)s_B^{-1}} \to 0 \; ,$$

$$\beta_+ \sim \mathrm{const} \; , \quad \beta_- \sim \mathrm{const}$$

and

$$\alpha_+ \sim \mathrm{const} \; , \quad \alpha_- \sim \mathrm{const} \; ,$$

$$\beta_+ \sim \epsilon^{-(\mu+\gamma/2)s_B^{-1}} \to \infty \; , \quad \beta_- \sim \epsilon^{1-(\mu+\gamma/2)s_B^{-1}} \to 0 \; ;$$

(iii) for $\mathrm{Re}(\mu) < -\gamma/2$,

$$\alpha_+ \sim \mathrm{const} \; , \quad \alpha_- \sim \mathrm{const} \; ,$$

$$\beta_+ \sim \epsilon^{-(\mu+\gamma/2)s_B^{-1}} \to 0 \; , \quad \beta_- \sim \epsilon^{1-(\mu+\gamma/2)s_B^{-1}} \to 0 \; .$$

A similar analysis may be performed near $x = M_A$, for which $s_A \equiv -f'(M_A) > 0$ and $\epsilon \equiv x - M_A \ll 1$. The results are similar except that s_A replaces s_B and $\alpha_\pm$ and $\beta_\pm$ replaces $\alpha_\mp$ and $\beta_\mp$, respectively. In case (ii) above, some eigenvectors components diverge at the boundary of the support. Nevertheless, the eigenvectors are normalizable.

C. Spectral representation of the rate kernel

In this subsection we obtain an expression for the spectral representation of the integrated rate kernel. Expand-

ing the auxiliary functions $\xi_i(x,t)$ [Eq. (2.23)] in terms of the right eigenfunctions of the projected evolution operator $Q\mathbf{D}$, we have

$$\xi_i(x,t) = \sum_\mu c_\mu \alpha_i^\mu(x) \exp(-\mu t) \; , \tag{2.35}$$

where c_μ is the expansion coefficient for mode μ. Using this expression in Eq. (2.22), performing the integrations, and using $f(x_0) = 0$, we obtain

$$K(t) = \sum_\mu d_\mu \exp(\mu t) \; , \tag{2.36}$$

where

$$d_\mu \equiv \Delta[\alpha_+^\mu(x_0) - \alpha_-^\mu(x_0)]c_\mu = \Delta Q c_\mu \tag{2.37}$$

are the rate spectral weights. To find the expansion coefficients c_μ, the orthogonality relation (2.33) is used together with the initial condition (2.24). We obtain

$$c_\mu = \sum_i \int_{M_A}^{M_B} dx \, \beta_i^\mu(x) p_{si}(x) u(x) = R \; . \tag{2.38}$$

For $\mu \neq 0$, the integration on the right-hand side of (2.38) can be easily performed by using the left-eigenvalue equations (2.31). The result is

$$c_\mu = R = \frac{k^{\mathrm{TST}}}{\mu} \{ \eta_A [\beta_+^\mu(x_0^+) - \beta_-^\mu(x_0^+)]$$

$$+ \eta_B [\beta_+^\mu(x_0^-) - \beta_-^\mu(x_0^-)]\}, \quad \mu \neq 0 \; . \tag{2.39}$$

Here

$$k^{\mathrm{TST}} \equiv \frac{\Delta}{2} p_s(x_0) \eta_A^{-1} \eta_B^{-1} \tag{2.40}$$

is the transition-state-theory rate [9]. The latter quantity is the phenomenological rate coefficient determined by considering the system initially located at the unstable fixed point and omitting the multiple reflexions across the potential barrier which may occur at later times. For $\mu = 0$ the eigenfunction can be obtained exactly and its contribution to the sum (2.36) easily determined. In the following, we omit the superscript μ on the eigenfunctions. Equations (2.36), (2.37), and (2.39) constitute the main results of this paper.

In the case for which the potential is symmetric $[V(x) = V(-x)]$, the eigenvectors are symmetric (or antisymmetric) with respect to a change of sign in both x and Δ:

$$\alpha_\pm(x) = \sigma \alpha_\mp(-x), \quad \beta_\pm(x) = \sigma \beta_\mp(-x) \; , \tag{2.41}$$

where $\sigma = +1$ or -1. In this case, only the odd eigenvectors ($\sigma = -1$) contribute to the rate kernel [see Eq. (2.37) with $x_0 = 0$].

D. The case $\mu = 0$

$\mu = 0$ is a doubly degenerate eigenvalue of the projected evolution operator. This property is also common to the

projected Fokker-Planck evolution operator [15]. Setting $\mu = 0$, it is easy to see by inspection that $\vec{\alpha} = (p_{s+}, p_{s-})$ and $\beta_+ = \beta_- = 1$ constitute one possible set of normalized eigenvectors consistent with $\beta_+(M_A)\beta_-(M_B)$ finite and $\alpha_+(M_A) = \alpha_-(M_B) = 0$. However, this solution does not contribute to the rate kernel (2.36) since $Q = p_{s+}(x_0) - p_{s-}(x_0) = 0$.

A linearly independent left eigenvector is simply $\beta_+ = \beta_- = \theta(x_0 - x) - \theta(x - x_0)$. The corresponding right eigenvector is found by solving Eq. (2.26). We find, after some algebra,

$$\alpha_+^0(x) = \frac{C}{2} p_s(x)[1 - f(x)/\Delta] + \frac{Q^0}{2} \int_{M_A}^x dx' p_s(x')u(x')$$
$$+ \frac{Q^0}{2} J(x)[1 - f(x)/\Delta] , \qquad (2.42)$$

$$\alpha_-^0(x) = \frac{C}{2} p_s(x)[1 + f(x)/\Delta] - \frac{Q^0}{2} \int_{M_A}^x dx' p_s(x')u(x')$$
$$+ \frac{Q^0}{2} J(x)[1 + f(x)/\Delta] , \qquad (2.43)$$

where C is a constant, $Q^0 = \alpha_+^0(x_0) - \alpha_-^0(x_0)$, and

$$J(x) \equiv -p_s(x)\Delta^{-1} \int_{x_0}^x dx' [1 - f^2(x')/\Delta^2]^{-1} \left[2f(x')u(x') + [f'(x') + \gamma]p_s^{-1}(x') \int_{M_A}^{x'} dy\, p_s(y)u(y) \right] .$$

The constant C is found by requiring the two $\mu = 0$ eigenvectors to be orthogonal: $\int_{M_A}^{M_B} dx (\alpha_+^0 + \alpha_-^0) = 0$, giving $C = -Q^0 \int_{M_A}^{M_B} J\, dx$. The normalization condition allows then the determination of Q^0:

$$Q^0 = \left\{ (\eta_B - \eta_A) \int_{M_A}^{M_B} dx\, J + \int_{M_A}^{x_0} dx\, J - \int_{x_0}^{M_B} dx\, J \right\}^{-1} . \qquad (2.44)$$

In the case of a symmetric potential, it is easy to see that $J(x) = -J(-x)$, so that $C = 0$.

This eigenfunction always contributes to the rate kernel (2.36). In particular, substituting $\beta_+ = \beta_- = \theta(x_0 - x) - \theta(x - x_0)$ in c_μ, the plateau value of the integrated rate kernel is obtained,

$$K(\infty) = d_0 = 2\Delta Q^0 . \qquad (2.45)$$

E. The case $\mu = -\gamma$

It is also straightforward to verify that $\mu = -\gamma$ is an eigenvalue. Setting $\beta_-(M_B) = \beta_+(M_A) = 0$, we obtain, from Eq. (2.31), for $x > x_0$,

$$\beta_+ = \frac{K_1}{2} \left\{ \exp \left[-\int_{x_0}^x dx' \gamma f/(f^2 - \Delta^2) \right] \right.$$
$$\left. + \frac{\gamma}{2k^{TST}\eta_A} \left[1 - \eta_B^{-1} \int_{x_0}^x p_s dx' \right] \right\} , \qquad (2.46)$$

$$\beta_- = \frac{K_1}{2} \left\{ \exp \left[-\int_{x_0}^x dx' \gamma f/(f^2 - \Delta^2) \right] \right.$$
$$\left. - \frac{\gamma}{2k^{TST}\eta_A} \left[1 - \eta_B^{-1} \int_{x_0}^x p_s dx' \right] \right\} , \qquad (2.47)$$

whereas for $x < x_0$,

$$\beta_+ = \frac{K_2}{2} \left\{ \exp \left[-\int_{x_0}^x dx' \gamma f/(f^2 - \Delta^2) \right] \right.$$
$$\left. - \frac{\gamma}{2k^{TST}\eta_B} \left[1 + \eta_A^{-1} \int_{x_0}^x p_s dx' \right] \right\} , \qquad (2.48)$$

$$\beta_- = \frac{K_2}{2} \left\{ \exp \left[-\int_{x_0}^x dx' \gamma f/(f^2 - \Delta^2) \right] \right.$$
$$\left. + \frac{\gamma}{2k^{TST}\eta_B} \left[1 + \eta_A^{-1} \int_{x_0}^x p_s dx' \right] \right\} . \qquad (2.49)$$

Here K_1 and K_2 are two integration constants. The first relation (2.32) gives a relationship between these constants: $\eta_B K_1 + \eta_A K_2 = 0$. With the help of Eq. (2.39), it is then easy to verify that the second relation (2.32) is identically verified, thus indicating that $-\gamma$ is indeed an eigenvalue.

III. AN EXACTLY SOLVABLE CASE: THE PIECEWISE QUADRATIC POTENTIAL

A. Model

In order to illustrate the formalism of the preceding section, we consider an example of bistable potential $V(x)$ which leads to an exactly solvable eigenvalue problem. The symmetric deterministic bistable potential has the generic normal form

$$V(x) = ax^4/4 - bx^2/2 , \qquad (3.1)$$

where a, b are positive coefficients. The deterministic evolution is then $\dot{x} = f(x) = bx - ax^3$. The deterministic fixed points are $x_0 = 0$ and $x_{A(B)} = -(+)\sqrt{b/a}$.

In this section we investigate a piecewise quadratic potential which represents a good approximation of the normal form. We nondimensionalize x by $\sqrt{b/a}$ and time by b^{-1}. Matching the curvature of the potential at the fixed points $(-1, 0, 1)$ we can write the simplified potential as
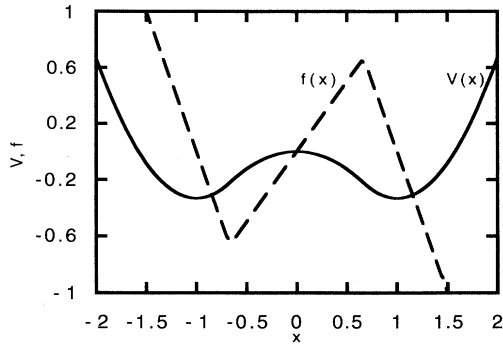
FIG. 1. Plots of the piecewise quadratic symmetric bistable potential in dimensionless units (continuous line) and the corresponding force (dashed line).

$$V(x) = \begin{cases} -X_2 + (x+1)^2, & x < -X_1 \\ -x^2/2, & |x| < X_1 \\ -X_2 + (x-1)^2, & x > X_1, \end{cases} \quad (3.2)$$

where the constants X_1, X_2 are found by continuity of V and V' at $|x| = X_1$: $X_1 = \frac{2}{3}$, $X_2 = \frac{1}{3}$ (Fig. 1). The dimensionless barrier height is $[V(0) - V(1)]\gamma/\Delta^2 = \gamma/(3\Delta^2)$. Our simplified model is therefore given by the following piecewise linear force:

$$\dot{x} = f(x) = -\frac{dV}{dx} = \begin{cases} -2x - 2, & x < -\frac{2}{3}, \\ x, & -\frac{2}{3} < x < \frac{2}{3}, \\ -2x + 2, & x > \frac{2}{3}. \end{cases} \quad (3.3)$$

The boundaries of the support are then $M_B = -M_A = 1 + \Delta/2$. It is easy to see that the condition $\Delta > \frac{2}{3}$ is required in order for the noise to bring the system out of its deterministic bistable regime and induce the transitions of interest here. The stationary density is then

$$p_s(x) = \begin{cases} Z[\Delta^2 - (2 - 2|x|)^2]^{\gamma/4 - 1}[\Delta^2 - \frac{4}{9}]^{-3\gamma/4}, \\ \qquad\qquad \frac{2}{3} < |x| < M_B, \\ Z(\Delta^2 - x^2)^{-\gamma/2 - 1}, \quad |x| < \frac{2}{3}. \end{cases} \quad (3.4)$$

In order for this stationary density to be bimodal, one must choose $\gamma > 4$ [Eq. (2.8) with $s_A = s_B = 2$].

B. The eigenvalue problem

With the expression (3.3) for the deterministic evolution, the eigenvalue problem (2.26) and (2.31) can be solved exactly. It is in fact simpler to solve the left eigenvalue problem (2.31) first. For each interval $x > 0$, $x < 0$

separately, the problem reduces to finding the left eigenvalue problem for the *unprojected* evolution operator, which was solved previously [14]. More explicitly, if we eliminate β_-, say, from Eq. (2.31), then for $x \neq 0$, β_+ must satisfy

$$\beta_+'' + \frac{\beta_+'}{f^2 - \Delta^2}[f(f' - \gamma - 2\mu) - \Delta f'] + \beta_+ \frac{\mu(\gamma + \mu)}{f^2 - \Delta^2} = 0. \quad (3.5)$$

Here the prime denotes differentiation with respect to x. Once β_+ is known, the other component is found from

$$\beta_- = \frac{2}{\gamma}[(\gamma/2 + \mu)\beta_+ - (f + \Delta)\beta_+']. \quad (3.6)$$

It is useful to introduce the change of variable

$$z = [1 - f(x)\Delta^{-1}]/2, \quad (3.7)$$

thus mapping the support onto the interval $[0,1]$. The point $x = -\frac{2}{3}$ corresponds to $z = z_1 \equiv \frac{1}{2} + 1/3\Delta$; similarly, $x = \frac{2}{3}$ corresponds to $z = z_2 \equiv \frac{1}{2} - 1/3\Delta$. As is easily verified, the solution for β_+ is given in terms of hypergeometric functions $F(a,b,c;z)$. The exact solution is explicitly given in Appendix A and involves eight constants a_i $(i = 1-8)$ (one of them being arbitrary).

The boundary conditions at $z = 0, 1$ are determined by the behavior of the eigenfunctions close to the support. Four more boundary conditions are obtained by continuity of the left eigenfunctions and its first derivative with respect to x at $x = \pm\frac{2}{3}$:

$$\beta_+(z = z_1^+) = \beta_+(z = z_1^-),$$
$$\beta_+(z = z_2^+) = \beta_+(z = z_2^-), \quad (3.8)$$

$$\beta_+'(z = z_1^+) + 2\beta_+'(z = z_1^-) = 0,$$
$$\beta_+'(z = z_2^-) + 2\beta_+'(z = z_2^+) = 0. \quad (3.9)$$

Here $z_1^\pm$ corresponds to $\lim_{\epsilon \to 0} x = -\frac{2}{3} \pm \epsilon$ and similarly $z_2^\pm$ corresponds to $\lim_{\epsilon \to 0} x = \frac{2}{3} \pm \epsilon$. The derivatives in (3.9) are with respect to z. Finally, the discontinuity conditions (2.32) provide two more boundary conditions at $z = \frac{1}{2}$. With these conditions, the constants a_i (one of them is arbitrary) and the eigenvalue μ can be found by solving a set of linear homogeneous equations. The left eigenvalue problem is thus solved.

The determination of the right eigenvector is slightly more involved. It is convenient to use the symmetry relation $\alpha_\pm(x) = -\alpha_\mp(-x)$ implied by the symmetry of the potential. In this case, $Q = 2\alpha_+(x = 0)$. Eliminating α_- from (2.26), using the definition of $p_{s\pm}$, p_s, and k^{TST}, we obtain after some algebra the following second-order inhomogeneous differential equation for α_+:

$$\alpha_+'' + \frac{\alpha_+'}{f^2 - \Delta^2}[f(3f' + \gamma + 2\mu) - \Delta f'] + \frac{\alpha_+}{f^2 - \Delta^2}[(f' + \mu)(f' + \mu + \gamma) + f''(f - \Delta)]$$

$$= Qu(x)\frac{p_s(x)}{2(f^2 - \Delta^2)(f + \Delta)}[\gamma(\Delta^2 + f^2) - (f^2 - \Delta^2)\mu - 2\Delta f'(f - \Delta)] - k^{TST}Q\delta(x)/\Delta. \quad (3.10)$$

Note that the right-hand side is *a priori* unknown since Q involves the value of α_+ at $x_0 = 0$.

The homogeneous part of this differential equation corresponds to the right eigenfunction equation for the *unprojected* evolution [14]. Again, the solution of the homogeneous equation is given in terms of hypergeometric functions. The solution of the inhomogeneous equation (3.10) can then be straightforwardly found. The explicit corresponding expressions are given in Appendix B and involve six unknown constants b_i ($i = 1-6$) (one of them being arbitrary).

The behavior of α_+ at $z = 0,1$ provides two boundary conditions. Two more boundary conditions are obtained by continuity of the eigenfunctions at $z = \pm\frac{2}{3}$:

$$\alpha_+(z = z_1^+) = \alpha_+(z = z_1^-),$$
$$\alpha_+(z = z_2^+) = \alpha_+(z = z_2^-),$$
(3.11)

Another boundary condition can be obtained by integrating the differential equation (3.10) across the discontinuity in f' at $z = -\frac{2}{3}$. One gets

$$\alpha_+'(z = z_1^+) + 2\alpha_+'(z = z_1^-) = 3\alpha_+(z = z_1)/z_2.$$
(3.12)

The corresponding boundary condition at $x = \frac{2}{3}$, $\alpha_+'(z = z_2^-) + 2\alpha_+'(z = z_2^+) = 3\alpha_+(z = z_2)/z_1$, is automatically satisfied when the proper eigenvalue μ is used. Using $Q = 2\alpha_+(z = \frac{1}{2})$, these conditions are sufficient to reduce the determination of the constants b_i to the solution of a set of linear inhomogeneous equations. α_- is then found through the symmetry relation (2.41) (with $\sigma = -1$). The determination of the right eigenvector is then complete up to an overall multiplicative constant, which may be found from the normalization condition (2.33).

Finally, for $\mu = 0$, the expressions (2.42)–(2.44) with $C = 0$ are used.

C. Results and discussion

The determination of the complete solution of the eigenvalue problem can be straightforwardly carried out with the help of a symbolic manipulation software. For illustrative purpose, we consider here two choices of the noise parameters Δ, γ. We recall that the deterministic (i.e., "molecular") time scale is $b^{-1} \equiv 1$ [see Eq. (3.3)].

In the first case $\Delta = 1$, $\gamma = 20$, giving $k^{TST} = 3.64123 \times 10^{-4}$. The barrier height is $\frac{20}{3} \approx 6.67$. Table I shows the first few eigenvalues which contribute to the rate kernel and the rate spectral weights d_μ. Figures 2(a) and 2(b) illustrate the first three normalized eigenfunctions α_+ and β_+. α_- and β_- may be obtained from these by using the symmetry relation (2.41) with $\sigma = -1$. From (2.45), we obtain the plateau value of the rate kernel $K(\infty) = 6.418 \times 10^{-5}$, which is much smaller than the first nonzero eigenvalue $\mu_1 = -2.2469$. This
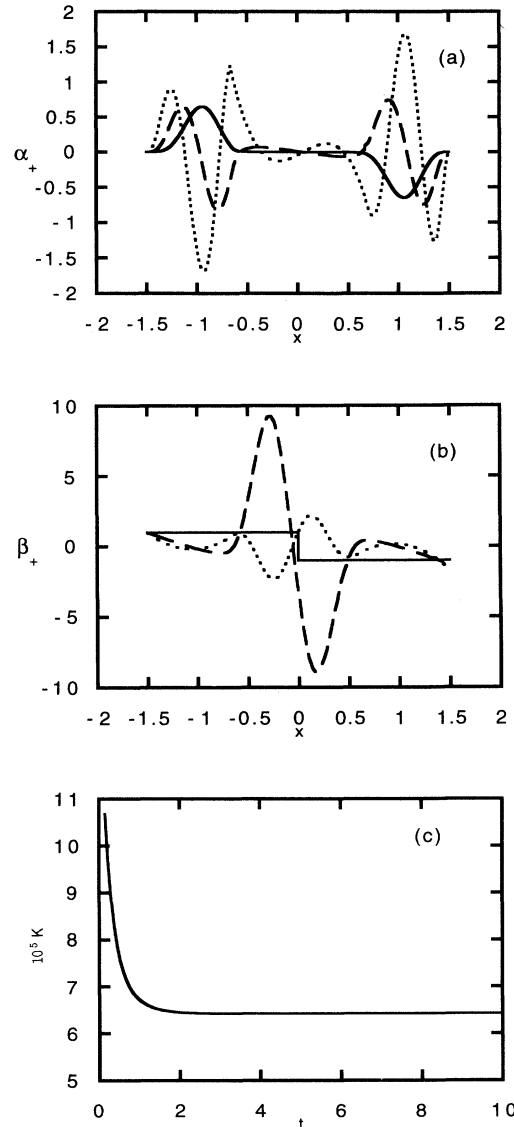

FIG. 2. The first three normalized eigenfunctions of the projected stochastic operator and the integrated rate kernel for the piecewise quadratic potential with $\Delta = 1$, $\gamma = 20$ (high barrier). For both (a) and (b) $\mu = 0$ (continuous line), $\mu = -2.2469$ (dashed line), and $\mu = -4.0038$ (dotted line). (a) Right eigenfunctions α_+; (b) left eigenfunctions β_+; (c) integrated rate kernel K.

TABLE I. The first few eigenvalues and spectral weights contributing to the integrated rate kernel for the piecewise quadratic symmetric potential. The first two columns correspond to $\Delta = 1$, $\gamma = 20$, the last two to $\Delta = 5$, $\gamma = 20$.

μ	$10^5\, d_\mu$	μ	d_μ
0	6.4180	0	0.5245
-2.2469	2.3757	-3.6564	0.2041
-4.0038	1.7305	-7.2814	0.2132
-5.7398	3.2105	-8.7827	-0.1223
-8.2426	2.8799	-12.7186	-0.1965
-11.7573	-3.3810	-16.3436	-0.2041

case presents a clear separation of time scales and we expect a phenomenological rate law to be valid with a phenomenological rate coefficient equal to $k = K(\infty)$ and a "transmission coefficient" $k/k^{\mathrm{TST}} = 0.1762$ [9]. Figure 2(c) gives the plot of the integrated rate kernel as a function of time. This plot is valid for times longer than the inverse of the absolute value of the smallest eigenvalue considered in the summation (2.36): $t > 0.085$. It is seen that the rate kernel quickly reaches its plateau value k in a time scale $\sim 1/|\mu_1|$ comparable to the deterministic

time scale, but short compared to the transition relaxation time $1/k$.

In the second case, $\Delta = 5$, $\gamma = 20$, giving $k^{\mathrm{TST}} = 2.0254$. The barrier height equals $\frac{4}{15} \approx 0.27$ and is much lower than in the first case. Again Table I gives the first few contributing eigenvalues and the rate spectral weights. Figures 3(a) and 3(b) illustrate the first three normalized eigenfunctions and Fig. 3(c) shows a plot of the integrated rate kernel as a function of time. This plot is valid for $t > 0.06$. The plateau value is $K(\infty) = 0.5245$. However, in contrast to the previous case, $K(\infty)$, $|\mu_1| = 3.6564$, and the inverse of the deterministic time scale (unity) all have the same order of magnitude. In this case, a simple phenomenological law is not valid and the behavior of the rate kernel $K(t)$ must be considered to establish the kinetics of the transition. Finally, although none were found in practice, it is possible that complex eigenvalues occurring in conjugate pairs exist.

The case of a nonsymmetric piecewise quadratic potential may also be straightforwardly investigated in a similar manner.

IV. QUARTIC POTENTIAL: A NUMERICAL APPROACH

The simplest bistable potential with continuous derivatives to all orders is the quartic potential $V(x) = ax^4/4 - bx^2/2 + cx$, with a and b positive. In this section, we numerically solve the eigenvalue problem for the projected dynamics in a symmetric potential ($c = 0$). In this case, it is sufficient to solve the problem on the interval $[M_A, 0]$ or $[0, M_B]$ and the symmetry relation (2.41) with $\sigma = -1$ can be used. The generalization of the algorithm to the case $c \neq 0$ is straightforward. Scaling x by $\sqrt{b/a}$ and time by b^{-1}, the deterministic potential and the force become

$$V(x) = x^4/4 - x^2/2, \quad f(x) = x - x^3 . \tag{4.1}$$

The dimensionless barrier height is then $\gamma/4\Delta^2$.

A. Numerical algorithm

We first consider the case $\mathrm{Re}(\mu) > 2 - \gamma/2$ or $-\gamma/2 < \mathrm{Re}(\mu) < 2 - \gamma/2$ (first solution family). From the asymptotic analysis of the behavior of the left eigenfunctions near M_A, we expect $\beta_i(M_A)$ to be a nonzero constant. $\beta_+(M_A)$ is arbitrarily set equal to unity. Evaluating Eq. (2.31) at M_A gives $\beta_-(M_A) = \gamma/(2\mu + \gamma)$. For a given value of the eigenvalue μ and with these initial conditions, the system of differential equations (2.31) is then numerically solved until $\beta_\pm(0^-)$ are obtained. Using the jump conditions (2.32) with (2.39), together with the symmetry relation (2.41), it is seen that the following relation is true:

$$\beta_+(0^-) = \beta_-(0^-) \frac{k^{\mathrm{TST}} + \mu}{k^{\mathrm{TST}} - \mu} \tag{4.2}$$

if μ is a proper eigenvalue. The value of μ is then changed and the procedure iterated until relation (4.2) is obtained within a tolerance limit.

For the case $-\gamma/2 < \mathrm{Re}(\mu) < 2 - \gamma/2$ (second solution
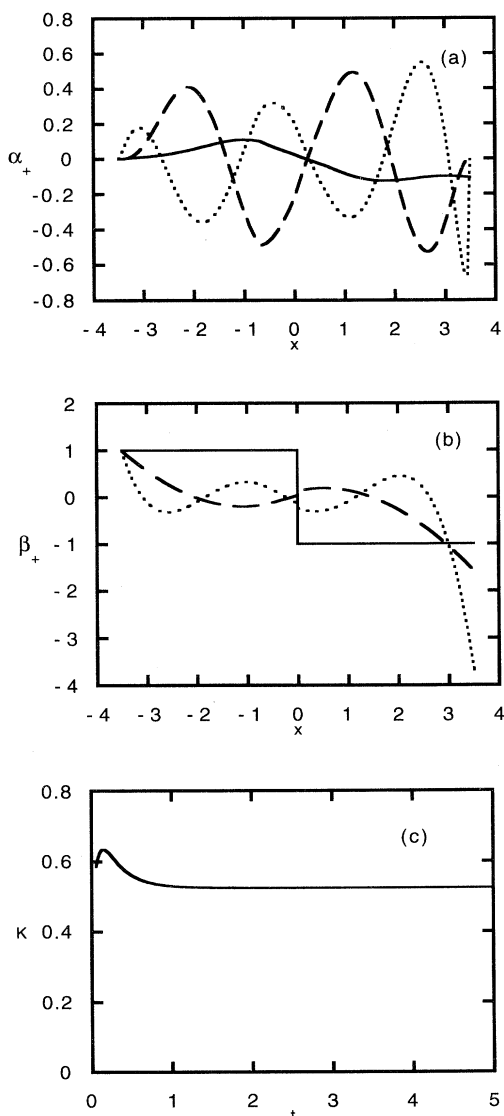

FIG. 3. The first three normalized eigenfunctions of the projected stochastic operator and the integrated rate kernel for the piecewise quadratic potential with $\Delta = 5$, $\gamma = 20$ (low barrier). For both (a) and (b) $\mu = 0$ (continuous line), $\mu = -3.6564$ (dashed line), and $\mu = -7.2814$ (dotted line). (a) Right eigenfunctions α_+; (b) left eigenfunctions β_+; (c) integrated rate kernel K.

family) or $\mathrm{Re}(\mu) < -\gamma/2$, one expects $\beta_-(M_B)$ to be zero. We arbitrarily set $\beta_+(0^+)=1$. Using (2.32) with (2.39) and the symmetry relation, one obtains $\beta_-(0^+)=(k^{\mathrm{TST}}+\mu)/(k^{\mathrm{TST}}-\mu)$. With these initial conditions, the system (2.31) is solved and the eigenvalue μ adjusted until $\beta_-(M_B)$ is zero within a tolerance limit.

In both cases, we obtain the right eigenfunctions in the following way. We arbitrarily set $\alpha_+(0)=1$. The symmetry condition (2.41) gives $\alpha_-(0)=-1$, so that $Q=2$. With these initial conditions, the system (2.26) is then

solved until $\alpha_{\pm}(M_B)$ is obtained. Finally, the overall normalization constant is determined by numerical integration of $\alpha_+\beta_+ + \alpha_-\beta_-$ [see (2.33)].

The differential equation solver uses a fifth-order Runge-Kutta method with adaptive step size. The value of $p_s(x)$ that appears on the right-hand side of (2.26) is obtained by numerical integration using Simpson's rule. Our algorithm is general and can be applied to other types of bistable potentials. The algorithm was verified by comparing its results for the piecewise quadratic po-
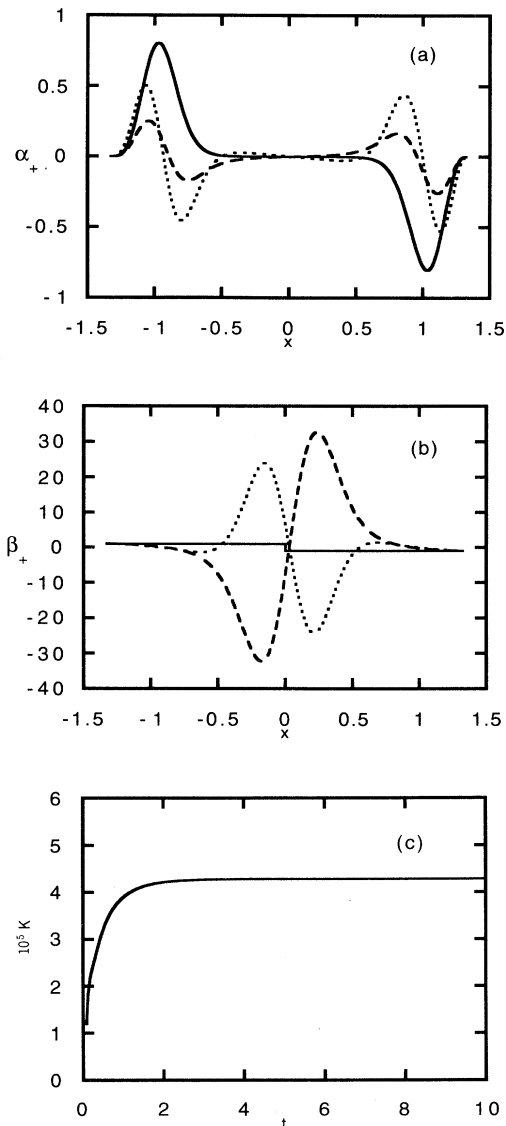

FIG. 4. The first three real normalized eigenfunctions of the projected stochastic operator and the integrated rate kernel for the quartic symmetric potential with $\Delta=1$, $\gamma=33$ (high barrier). For both (a) and (b) $\mu=0$ (continuous line), $\mu=-1.3702$ (dashed line), and $\mu=-1.9214$ (dotted line). (a) Right eigenfunctions α_+; (b) left eigenfunctions β_+; (c) integrated rate kernel K.
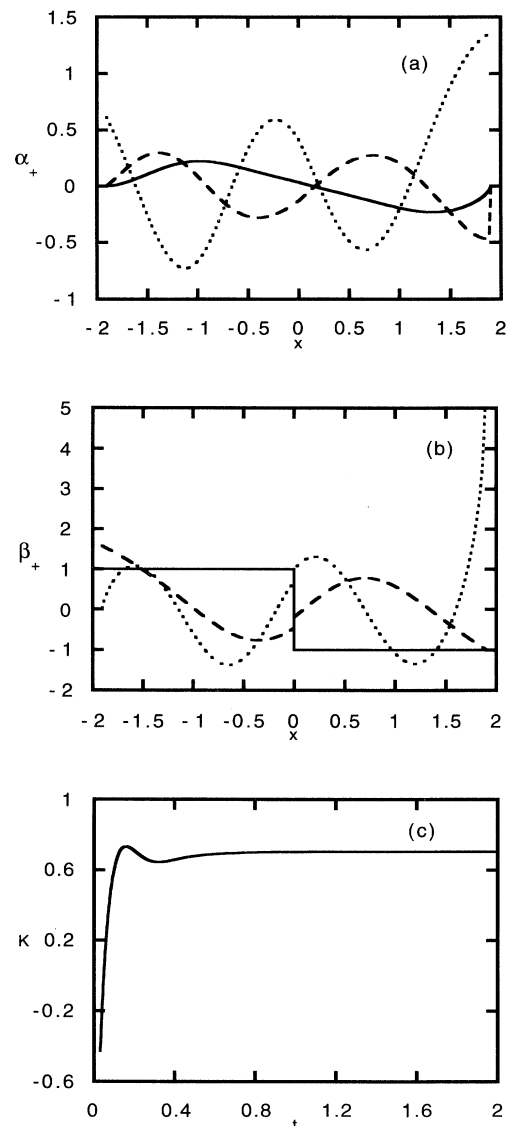

FIG. 5. The first three real normalized eigenfunctions of the projected stochastic operator and the integrated rate kernel for the quartic symmetric potential with $\Delta=5$, $\gamma=33$ (low barrier). For both (a) and (b) $\mu=0$ (continuous line), $\mu=-5.9972$ (dashed line), and $\mu=-14.1378$ (dotted line). (a) Right eigenfunctions α_+; (b) left eigenfunctions β_+; (c) integrated rate kernel K.

IVAN L'HEUREUX

TABLE II. The first few eigenvalues and spectral weights contributing to the integrated rate kernel for the quartic symmetric potential. The first two columns correspond to $\Delta=1$, $\gamma=33$, the last two to $\Delta=5$, $\gamma=33$.

μ	$10^5 d_\mu$	μ	d_μ
0	4.284	0	0.704
-1.3702	-0.664	-5.9972	-0.353
-1.9214	-1.158	$-7.8909\pm5.8367i$	$0.206\mp0.240i$
-3.1284	-1.184	$-8.3173\pm10.4670i$	$0.037\mp0.094i$
-4.7141	-0.038	$-8.8185\pm14.4400i$	$-0.082\mp0.046i$
-6.8061	-1.253	$-9.0215\pm17.9368i$	$-0.057\mp0.060i$
-9.5927	-1.256	-14.1378	-1.250
$-12.7574\pm2.3138i$	$-0.291\mp1.149i$	-27.0028	-0.437
$-13.2493\pm4.3013i$	$-0.149\mp1.412i$	-33	-0.704
$-13.3619\pm6.0946i$	$0.313\mp1.221i$		
$-13.4468\pm7.8783i$	$0.218\mp0.700i$		
$-13.5653\pm9.5245i$	$-0.050\mp0.980i$		
-13.6774	-1.238		
-19.3226	-3.320		

tential with the exact results of Sec. III: they were undistinguishable.

B. Results and discussion

Two values of the noise parameters are adopted in this study such that k^{TST} is comparable to the values obtained for the two piecewise quadratic potential cases.

In the first case, $\Delta=1$, $\gamma=33$, giving $k^{\mathrm{TST}} = 3.1855\times10^{-4}$ and $-M_A=M_B=1.3247179$. The barrier height is $\frac{33}{4}=8.25$. Table II shows the first few eigenvalues and the rate spectral weights d_μ which contribute to the integrated rate kernel. Figures 4(a) and 4(b) illustrate the first three normalized real eigenfunctions. In contrast to the piecewise quadratic potential case, there exist complex eigenvalues. The search in the complex μ plane was limited to low frequencies [$|\mathrm{Im}(\mu)|<10$]. Figure 4(c) shows the plot of the integrated rate kernel as a function of time. This plot is valid for $t>1/\mathrm{Re}(-\mu)_{\max}=0.052$. On the scale of the plot, the complex spectral weights do not show any significant effect as their contribution is small. The plateau value of the rate kernel $K(\infty)=4.284\times10^{-5}$, which is much smaller than the first nonzero eigenvalue $\mu_1=-1.3702$. As in Sec. III, this case presents a clear separation of time scales. The phenomenological rate transmission coefficient is $k/k^{\mathrm{TST}}=K(\infty)/k^{\mathrm{TST}}=0.1345$.

In the second case, $\Delta=5$, $\gamma=33$, giving $k^{\mathrm{TST}}=2.48653$ and $-M_A=M_B=1.9041608$. The barrier height is low and is equal to 0.33. Again Table II gives the first few contributing eigenvalues and the rate spectral weights. Complex eigenvalues are found and their search was limited to low frequencies [$|\mathrm{Im}(\mu)|<20$]. Figures 5(a) and 5(b) show the first three normalized real eigenfunctions and Fig. 5(c) gives the plot of $K(t)$. This plot is valid for $t>0.03$. The plateau value is $K(\infty)=0.704$. Again, as in the low barrier piecewise quadratic potential case, a simple phenomenological law is not valid. Another feature to be observed is the presence of oscillations in $K(t)$ reflecting the multiple barrier crossings under rapid stochastic dynamics. Of all the complex eigenvalues, those with the three smallest imaginary parts dominate the contribution to $K(t)$. Thus the contribution of higher frequency components $|\mathrm{Im}(\mu)|>20$ is expected to be negligible.

V. CONCLUSION

In this paper, we presented a formalism for the study of the kinetics of dichotomous noise-induced transitions in a bistable system. Population numbers are associated with the number of phase points evolving under stochastic dynamics within a deterministic basin of attraction. Assuming completeness of the eigenfunctions of the projected stochastic operator $Q\mathbf{D}$, we used spectral methods to determine the integrated rate coefficient and to investigate the memory effects in the decay of the population number.

For two values of the noise parameters, this analysis was carried out exactly for a symmetric piecewise quadratic potential and numerically for a symmetric quartic potential. For each potential, one case corresponded to a high barrier potential, for which a phenomenological rate law is obtained. The value of the rate coefficient is determined. The other case referred to a low barrier, for which the population number relaxation time scale is not very different from the time scale of the dynamics inside the well. The memory effects are then important.

An asymptotic analysis has shown [6] that the decay of the population number may develop an algebraic tail in

some special cases. To properly account for this behavior, the continuous part of the spectrum should be obtained, if it exists. However, the explicit determination of such a continuous spectrum is still a challenge in general.

The numerical approach presented here can be straightforwardly generalized to an arbitrary bistable potential. Possible extensions of this work would be to bistable systems described by the dynamics of two variables or to rate processes induced by multiplicative dichotomous noise.

APPENDIX A

In this appendix we explicitly write the left eigenfunction β_+ for the piecewise quadratic potential. Changing the variable in (3.5) from x to z, as defined by (3.7), it is easy to obtain the solution as a function of z:

$$\beta_+(z) = \begin{cases} a_1 F(\mu/2, \mu/2+\gamma/2, \mu/2+\gamma/4; z) + a_2 z^{1-\gamma/4-\mu/2} F(1+\gamma/4, 1-\gamma/4, 2-\gamma/4-\mu/2; z) & \text{for } 0 < z < z_1 \\ a_3 F(-\mu, -\mu-\gamma, -\mu-\gamma/2; z) + a_4 z^{1+\gamma/2+\mu} F(1-\gamma/2, 1+\gamma/2, 2+\gamma/2+\mu; z) & \text{for } \frac{1}{2} < z < z_1 \\ a_5 F(-\mu, -\mu-\gamma, -\mu-\gamma/2; z) + a_6 z^{1+\gamma/2+\mu} F(1-\gamma/2, 1+\gamma/2, 2+\gamma/2+\mu; z) & \text{for } z_2 < z < \frac{1}{2} \\ a_7 F(\mu/2, \gamma/2+\mu/2, 1+\gamma/4+\mu/2; 1-z) \\ \qquad a_8 (1-z)^{-\gamma/4-\mu/2} F(\gamma/4, -\gamma/4, 1-\gamma/4-\mu/2; 1-z) & \text{for } z_2 < z < 1 \ . \end{cases} \tag{A1}$$

Here a_i ($i = 1$–8) are constants to be determined, $z_1 \equiv \frac{1}{2} + 1/3\Delta$, $z_2 \equiv \frac{1}{2} - 1/3\Delta$, and the four ranges in (A1) correspond to $x < -\frac{2}{3}$, $-\frac{2}{3} \leq x < 0$, $0 < x \leq \frac{2}{3}$, and $x > \frac{2}{3}$, respectively.

The asymptotic behavior of β_+ presented in Sec. II B implies the following choices.

(i) For $\mu > 2 - \gamma/2$ or $-\gamma/2 < \mu < 2 - \gamma/2$ (first solution family), $\beta_+(z=0)$ and $\beta_+(z=1)$ are constants. In this case, $a_2 = a_8 = 0$. We also arbitrarily set $a_1 = 1$.

(ii) For $-\gamma/2 < \mu < 2 - \gamma/2$ (second solution family) or

$\mu < -\gamma/2$, $\beta_+(z=0) = 0$, implying $a_1 = 0$. Finally, from the behavior of β_+ about $z = 1$, we set $a_7 = 0$. We also arbitrarily set $a_2 = 1$.

APPENDIX B

In this appendix we explicitly write the right eigenfunction α_+ for the piecewise quadratic potential. The starting point is the inhomogeneous differential equation (3.10). It is easy to obtain the regular solution α_+^H of its homogeneous counterpart as a function of z:

$$\alpha_+^H(z) = \begin{cases} b_1 F(1-\mu/2, 1-\mu/2-\gamma/2, 1-\mu/2-\gamma/4; z) + b_2 z^{\gamma/4+\mu/2} F(1-\gamma/4, 1+\gamma/4, 1+\gamma/4+\mu/2; z) & \text{for } 0 < z < z_1 \\ b_3 F(1+\mu, 1+\gamma+\mu, 1+\gamma/2+\mu; z) + b_4 z^{-\gamma/2-\mu} F(1+\gamma/2, 1-\gamma/2, 1-\gamma/2-\mu; z) & \text{for } z_2 < z < z_1 \\ b_5 F(1-\mu/2, 1-\gamma/2-\mu/2, 2-\gamma/4-\mu/2; 1-z) \\ \qquad + b_6 (1-z)^{-1+\gamma/4+\mu/2} F(\gamma/4, -\gamma/4, \gamma/4+\mu/2; 1-z) & \text{for } z_2 < z < 1 \ . \end{cases} \tag{B1}$$

Here b_i ($i = 1$–6) are constants to be determined (one of them being arbitrary).

The particular solution of (3.10) α_+^P is easily found to be

$$\alpha_+^P(x) = y_1(x) \int_{M_A}^x dx \, h(x) y_2(x) W(x)^{-1} - y_2(x) \int_{M_A}^x dx \, h(x) y_1(x) W(x)^{-1} , \tag{B2}$$

where $y_{1,2}(x)$ are the two linearly independent solutions of the homogeneous equation [read off Eq. (B1)], $h(x)$ denotes the inhomogeneous term on the right-hand side of (3.10), and $W(x) \equiv (dy_1/dx) y_2 - (dy_2/dx) y_1$ is the

Wronskian. To obtain the complete solution, we perform the change of variable $z = [1 - f(x)/\Delta]/2$ in (B2) and add the resulting solution $\alpha_+^P(z)$ to $\alpha_+^H(z)$.

The asymptotic behavior of α_+, discussed in Sec. II B implies the following choices.

(i) For $\mu > 2 - \gamma/2$ or $-\gamma/2 < \mu < 2 - \gamma/2$ (first solution family), $\alpha_+(z=0) = 0$, implying $b_1 = 0$. Finally, from the behavior of α_+ about $z = 1$, we set $b_5 = 0$. We also arbitrarily set $b_2 = 1$.

(ii) For $-\gamma/2 < \mu < 2 - \gamma/2$ (second solution family) or $\mu < \gamma/2$, $\alpha_+(z=0)$ and $\alpha_+(z=1)$ are constants. In this case, $b_2 = b_6 = 0$. We also arbitrarily set $b_1 = 1$.

[1] C. M. Bowden, M. Clifton, and H. R. Robb, *Optical Bistability* (Plenum, New York, 1982).

[2] *Oscillations and Traveling Waves in Chemical Systems*, edited by R. Field and M. Burger (Wiley, New York, 1985).

[3] A. T. Winfree, *The Geometry of Biological Time* (Springer, New York, 1980).

[4] W. Horsthemke and R. Lefever, *Noise-Induced Transitions. Theory and Applications in Physics, Chemistry and Biology* (Springer, Berlin, 1984).

[5] *Noise in Nonlinear Dynamical Systems*, edited by F. Moss and P. V. E. McClintock (Cambridge University Press, Cambridge, 1988).

[6] I. L'Heureux and R. Kapral, J. Chem. Phys. **88**, 7468 (1988).

[7] I. L'Heureux, R. Kapral, and K. Bar-Eli, J. Chem. Phys. **91**, 4285 (1989).

[8] I. L'Heureux, Phys. Lett. A **171**, 204 (1992).

[9] I. L'Heureux and R. Kapral, J. Chem. Phys. **90**, 2453 (1989).

[10] P. Hänggi and P. Riseborough, Phys. Rev. A **27**, 3379 (1983).

[11] C. Van den Broeck and P. Hänggi, Phys. Rev. A **30**, 2730 (1984).

[12] J. M. Porrá, J. Masoliver, and K. Lindenberg, Phys. Rev. A **44**, 4866 (1991).

[13] J. M. Porrá, J. Masoliver, K. Lindenberg, I. L'Heureux, and R. Kapral, Phys. Rev. A **45**, 6092 (1992).

[14] I. L'Heureux, in *Fluctuations and Order,* edited by M. Millonas (Springer, New York, 1994).

[15] X.-G. Wu and R. Kapral, J. Chem. Phys. **91**, 5528 (1989).

[16] X.-G. Wu, I. L'Heureux, and R. Kapral, Chem. Phys. Lett. **176**, 242 (1991).

[17] X.-G. Wu and I. L'Heureux, Chem. Phys. Lett. **191**, 463 (1992).

[18] K. Kitahara, W. Horsthemke, and R. Lefever, Phys. Lett. **70A**, 377 (1979).

[19] J. M. Sancho and M. San Miguel, Prog. Theor. Phys. **69**, 1085 (1983).

[20] F. Sagués, M. San Miguel, and J. M. Sancho, Z. Phys. B **55**, 269 (1984).